Available online at www.sciencedirect.com
SCIENCE DIRECT®
Remote Sensing of Environment 84 (2003) 589–602
Remote Sensing of Environment
www.elsevier.com/locate/rse

Spatial analysis of radiometric fractions from high-resolution multispectral imagery for modelling individual tree crown and forest canopy structure and health

Josée Lévesque[a,*], Douglas J. King[b]

[a] Defense Research and Development Canada-Valcartier, 2459 PIE-XI North Boulevard, Val-Bélair, Quebec, Canada G3J 1X5
[b] Department of Geography and Environmental Studies, Carleton University, 1125 Colonel By Drive, Ottawa, Ontario, Canada K1S 5B6

Received 15 April 2002; received in revised form 23 October 2002; accepted 26 October 2002

Abstract

Research was conducted in a forest adjacent to an abandoned acid mine tailings site to assess forest structural health using high spatial and spectral resolution digital camera imagery. Conventional approaches to this problem involve the use image spectral information, basic spectral transformations, or occasionally spatial transformations of image brightness. This research introduces fractional textures and semivariance analysis of image fractions. They were integrated with conventional image measures in stepwise multiple regression modelling of forest structure (canopy and crown closure, stem density, tree height, crown size) and health (a visual stress index). The goal was to conduct a relative comparison of the potential of the various image variable types in modelling of forest structure and health. Analysis was conducted for both canopy (crowns and shadows) and individual tree crown sample data sets extracted from 10 nm bandwidth spectral bands at three resolutions (0.25, 0.5, 1.0 m). Spatial transformations (texture, semivariogram range) of image brightness (DN) and image fractions (IF) were consistently the most significant and first entered variables in the best models of the forest parameters. At the canopy-scale, despite a limited number of available plots (6), stable models were produced that demonstrated the potential for spatially transformed variables. Semivariogram range explained 88% of the total variation of 9 of the 18 models and represented 56% of the variables used in all models while texture variables explained 51% of model variance in 8 of the 18 models and represented 40% of the variables used. At the tree crown scale ($n = 31$), 88% of the total variation of six of eight models was explained by texture variables and 6% by semivariogram variables. DN and IF variables that were not spatially transformed contributed little to the models at both scales. They represented 4% and 6%, respectively, of the variables used in all models. Spatial information in image fractions and image brightness has proven to be more significant than spectral information in these analyses. Of the spatial resolutions evaluated, 0.5 m consistently produced similar or better models than those using the 0.25 or 1.0 m resolutions. These results demonstrate the potential for integration of spatial transforms of image fractions and raw brightness in high-resolution modelling of forest structure and health.

Keywords: Airborne digital camera; Boreal forest structure and health; Image fractions; Image spatial analysis

1. Introduction

Stress in forests displays a variety of symptoms, some of which may be detected by remote sensing. Conventionally, change in leaf spectral reflectance has been the symptom studied. Increases in red reflectance due to reduced chlorophyll absorption, decreases in near infrared (NIR) reflectance from reduced cell vigor and shifts in the red edge between these two spectral regions have been commonly used as indicators of leaf stress (Carter, 1994; Curtiss & Ustin, 1989; Luther & Carroll, 1999; Merzlyak, Gitelson, & Zur, 1999; Salisbury & Ross, 1985). However, forest structural changes may be incurred due to disturbance over short periods (e.g., partial cutting, storm damage), or longer periods (e.g., contamination/pollution, climate change). Structural change may also be manifested at an individual crown scale or at the forest canopy scale. Image-based vegetation indices are commonly used as indicators of canopy chlorophyll content and vertical structure (e.g., leaf area index—LAI) to estimate forest canopy condition (Carlson & Ripley, 1997; McDonald, Gemmel, & Lewis, 1998; Pinty & Verstraete, 1992; Yoder & Waring, 1994).

* Corresponding author. Tel.: +1-418-844-4000x4301; fax: +1-418-844-4511.
E-mail address: josee.levesque@drdc-rddc.gc.ca (J. Lévesque).

0034-4257/02/$ - see front matter © 2002 Elsevier Science Inc. All rights reserved.
PII: S0034-4257(02)00182-7

However, vegetation indices do not behave linearly and saturate at low or high vegetation covers depending on the index used (Gamon et al., 1995; Turner, Cohen, Kennedy, Fassnacht, & Briggs, 1999). This limitation can be overcome using fraction images of cover types derived from spectral mixture analysis if enough bands are used to resolve the number of cover types present.

An image pixel spectrum can be modeled as a linear combination of pure reflectance components or endmember spectra. A fraction image or abundance image can be generated for each endmember (Boardman, 1995) in a process termed 'spectral mixture analysis' or 'spectral unmixing'. It is beyond the scope of this paper to describe all the methods of spectral mixture analysis that have been proposed, but the method applied in this study is given later in this paper. Example applications include determination of sub-pixel fractions of sunlit canopy, sunlit background and shadow to predict forest productivity parameters such as biomass, net primary productivity (NPP) and LAI (Peddle, Hall, & LeDrew, 1999), temporal analysis using endmember spectra representing forest change types derived from a multi-year sequence of NDVI values (Piwowar & Peddle, 1999), and integration of fractions with raw image data and image texture to predict forest structure (Peddle, Davidson, Johnson, & Hall, 1999). In these and other studies, spectral mixture analysis often provides better forest models than those obtained using only raw spectral data or vegetation indices.

Spatial image analysis of forest imagery has most commonly been conducted using texture and semivariance measures. Unlike pixel-by-pixel analysis, these techniques consider the spatial relationships between pixels (Atkinson & Lewis, 2000). Image texture information has often improved forest structure models (e.g., Wulder, Franklin, & Lavigne, 1996) and land cover classifications (e.g., Berberoglu, Lloyd, Atkinson, & Curran, 2000), and has been linked to site characteristics such as nutrient availability and microclimatic conditions (Coops & Culvenor, 2000). In semivariance analysis, the semivariogram parameters (range, sill, nugget) have been used to model Balsam fir damage (Bowers, Franklin, Hudak, & McDermid, 1994), map vegetation communities (Wallace, Watts, & Yool, 2000), and determine appropriate image resolution and sample plot size (Butson & King, 1999). Treitz and Howarth (2000) found that different scales of variability are present in a single spatial resolution that relate to ground (forest ecosystem class, contribution of understory) and sensor (wavelength) characteristics. Lévesque and King (1999), in a paper preceding this one, found strong relations with many of the forest structure and health parameters described here.

2. Research objectives

In this research, the benefits of both spectral unmixing and spatial image analysis described above are combined. Spatial analysis of spectrally unmixed image fractions is introduced and integrated with spectral and spatial image brightness characteristics. It was hypothesized that the spatial pattern and dependence of vegetation and shadow image fractions would significantly contribute to models of forest structure variation that are manifested in both individual crowns and over the forest canopy. Furthermore, since image fractions are essentially areal proportions of endmember types within a pixel, it was expected that they would provide complementary information to that derived from pixel brightness. The objectives were to investigate:

1. the relative potential of raw image brightness, spatial transformations of image brightness, image fractions derived from spectral mixture analysis, and spatial transformations of image fractions in modelling of forest structure and health parameters;
2. the influence of image spatial resolution and image sampling scale (i.e., image samples extracted over the forest canopy versus individual tree crown samples) on these models.

3. Study site

The study site (Fig. 1) was located in a forested area adjacent to, and downstream from, the abandoned Kam-Kotia copper–zinc mine about 40 km northwest of Timmins, Ontario. Important aspects of the site are summarized here; more detail is given in previous publications (Lévesque & King, 1999; Olthof & King, 2000; Walsworth & King, 1999). The forest is composed of mature trembling aspen (*Populus tremuloides*), a few small pockets of co-dominant balsam poplar (*Populus balsamifera*), and an understory of young black spruce (*Picea mariana*), white spruce (*Picea glauca*) and balsam fir (*Abies balsamea*). One of three large sulphide tailings areas of about 180 ha at the mine site was not impounded or controlled in any way during the 25 years preceding this study (Fig. 1). Surface drainage of low pH (1.4–2.0) and groundwater flow around and through the study area, resulting in elevated concentrations of some metals in surface soils and a decreasing gradient of these metals with increasing distance from the tailings (Lévesque & King, 1999). High winds that develop over the open tailings transport sulphide dust into the forest depositing it on leaves, branches and trunks. They also cause significant tree blow down and, in summer, increased evapotranspiration due to elevated tailings surface temperatures. All of these stress factors result in very dynamic forest conditions, particularly close to the tailings edge. Visible signs of forest damage include: (1) aspen leaf discolouration, lack of development to normal size, and curling; (2) thin and open aspen crowns with dead branches and clustered leaf distributions; (3) poor regen-

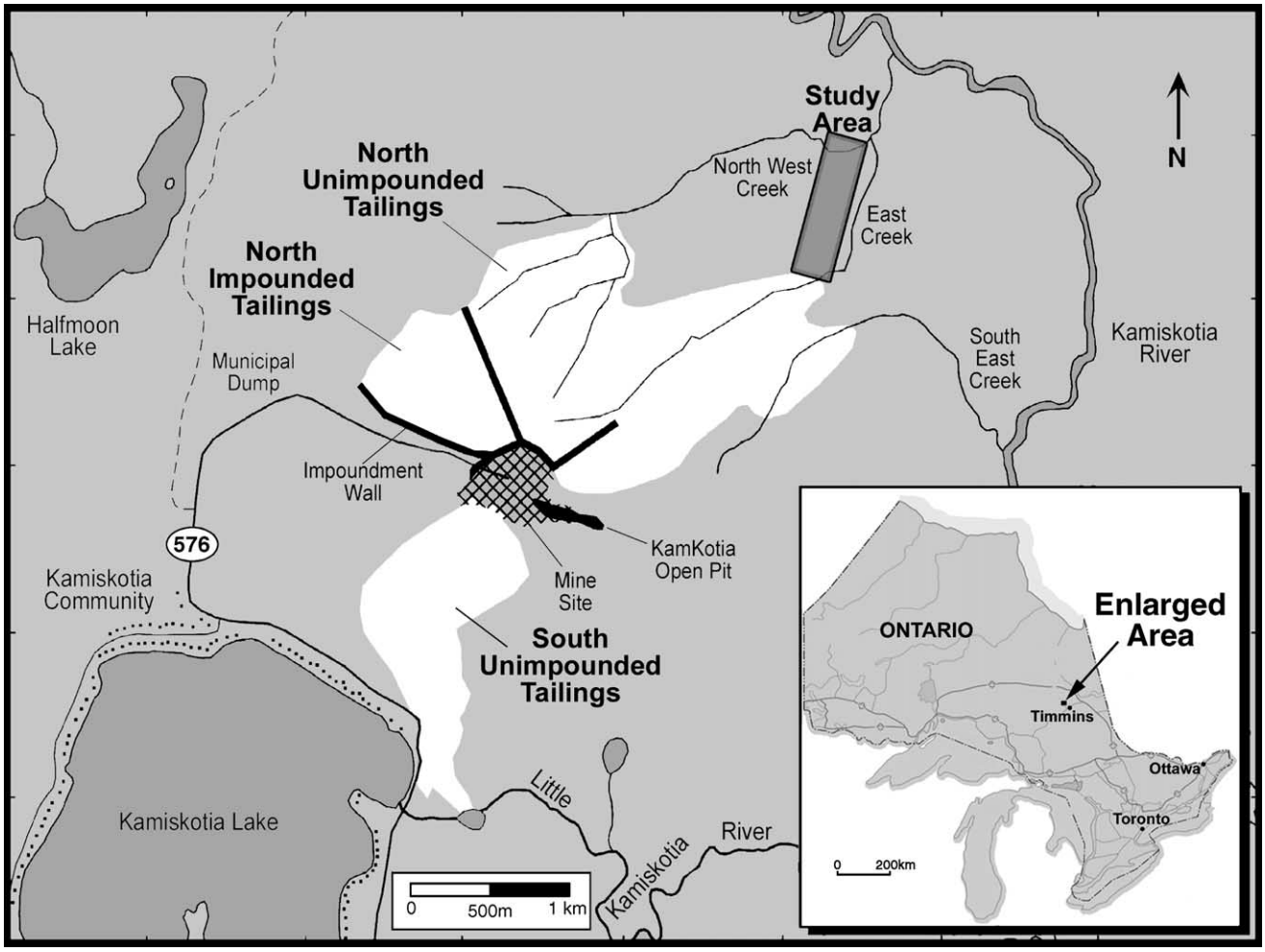

Fig. 1. Map of the KamKotia Mine showing the three tailings deposits and the study area (modified from Cosmopoulos, 2000).

eration on the forest floor; (4) standing dead trees; and (5) a large number of blown down trees. Walsworth and King (1999) evaluated the forest dynamics at the site using temporal aerial photography spanning the period from 1961, just after extensive tailings deposition began, to 1991. Using automated tree crown delineation techniques, and spatio-temporal transition modelling, they found a significant trend towards opening of the forest canopy and perpetuation of pioneer species over that time in an area within 200 m of the tailings edge. Further away, the trend was towards influx of later successional conifers. Thus, the area close to the tailings edge is in a constant state of disturbance from the factors described above. This spatial trend was confirmed using field measures of canopy closure, LAI, standing mortality and blowdown by Olthof and King (2000). Cosmopoulos and King (in press) found statistically significant changes in these forest structure parameters in the period of 1997–1999.

Six plots were established in 1993 along a transect traversing the forest at 40, 140, 240, 440, 640, and 840 m from the mine tailings and following the drainage direction (Fig. 2). The transect location was selected arbitrarily before field visits (using an air photo) to be in the central portion of a stand dominated by aspen. Similarly, the plot distances along the transect were selected arbitrarily without reference to the air photo and without field knowledge of the site. The furthest plot, plot 6, was located on slightly higher ground across the west/north creek and was expected not to be affected by the tailings. The initial goal was to sample and analyse individual trees in each plot based on research by King, Yuan, and Sankey (1992) on sugar maple decline. The plots were 50×50 to 60×60 m to obtain at least 30 dominant trees in each.

In previous remote sensing research at the study site, Olthof and King (1997), in a mixed wood area just west of this study area, found that combining co-occurrence texture (Haralick, Shanmugan, & Dinstein, 1973) and texture variation with spectral image brightness or vegetation indices significantly improved LAI models over those produced using spectral measures alone. Seed and King (2002), using the same field and image data, found that shadow brightness extracted from 0.25 m pixel digital camera imagery was a more robust predictor of mixed forest LAI over varying view angles than shadow fraction. Lévesque and King

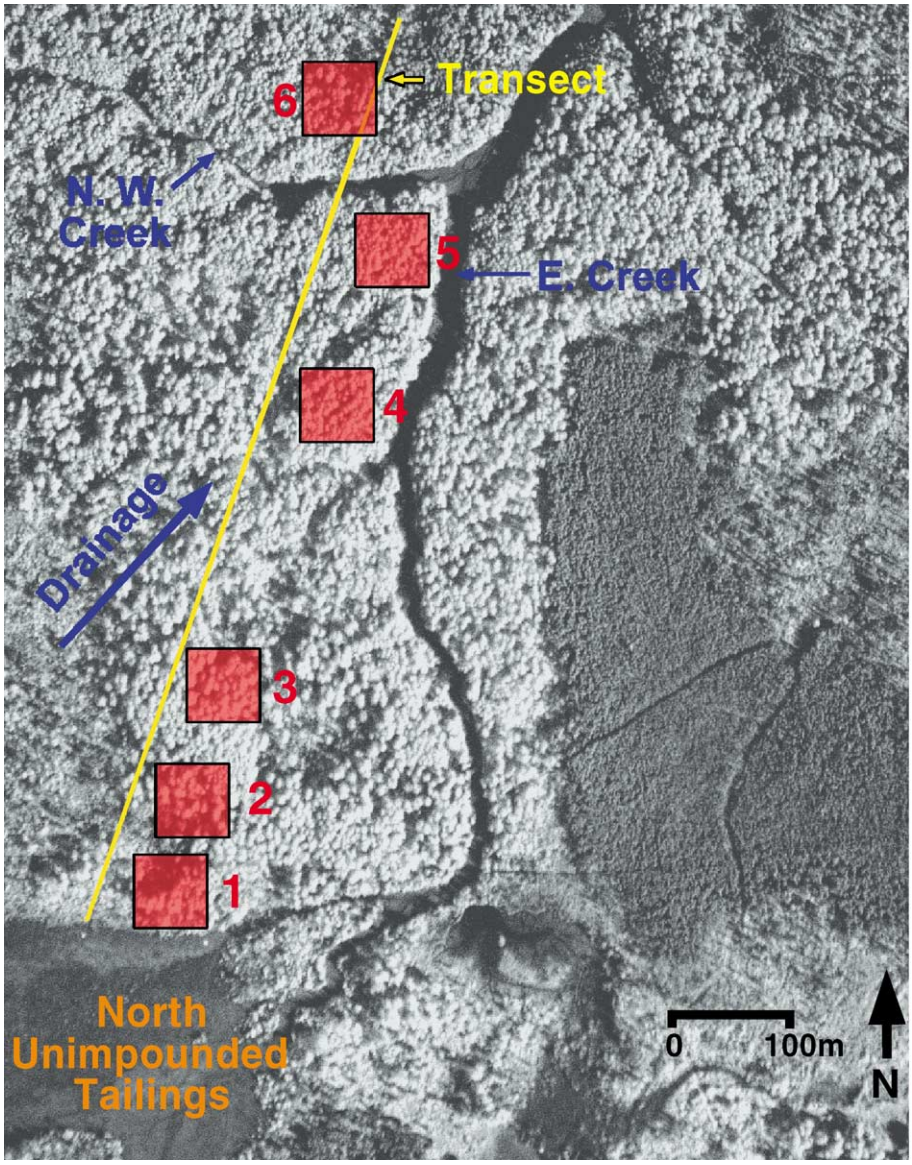

Fig. 2. Near-infrared digital camera image of the study site showing the study plot layout. Image from September 7, 1995. Pixel spacing is 1.0 m.

(1999), using forest and image data from the study presented here, found that semivariance range measures in high resolution near infrared imagery were highly correlated with individual crown closure, crown size, and forest canopy closure. From the experiences in the above studies of modelling individual forest variables, Olthof and King (2000) defined a multivariate forest structure condition index that can be measured and monitored using remote sensing spectral and spatial variables. They used canonical analysis to relate standing live, standing dead, and fallen (mostly blown down) forest structural measures to a set of spectral measures, textural measures and whole pixel radiometric fractions derived from image cluster analysis. This methodology was refined in Cosmopoulos and King (in press) and applied in temporal analysis of forest change for the 1997–1999 period.

4. Methods

4.1. Forest measurements

A total of 180 trees (30 in each plot) were sampled for six forest canopy and individual tree variables, which describe the structure and health characteristics of each of the plots. The six variables were: (1) forest canopy closure in percent, (2) forest stem density as number of trees per 100 m^2, (3) tree crown diameter in metres, (4) tree height in metres, (5) individual tree crown closure in percent, and (6) a tree stress index ranging from 1 to 5, where 1, 2, 3, and 4 represent no, slight, moderate, and severe damage, and 5 represents a dead tree. More detail on the measurement methods and analysis of these forest variables is given in Lévesque and King (1999). Table 1

Table 1
Average (avg) and standard deviation (std) of forest canopy and tree variables for each plot

		Plot					
		1	2	3	4	5	6
Forest canopy closure (%)	avg	40.83	40.00	56.67	50.00	66.67	55.00
	std	25.23	16.90	11.06	17.89	9.43	18.71
Forest stem density (per 100 m^2)	avg	7.33	5.50	5.60	9.20	18.25	16.43
	std	1.89	2.14	2.80	1.83	3.90	6.84
Tree crown size (m)	avg	6.42	7.79	8.14	5.54	5.43	6.38
	std	1.37	1.86	1.93	1.49	1.24	2.25
Tree height (m)	avg	26.88	26.60	30.32	24.58	24.93	25.67
	std	1.90	2.68	3.37	3.04	3.27	6.12
Tree crown closure (%)	avg	62.30	67.00	62.40	72.30	63.70	59.00
	std	10.90	10.70	11.80	9.37	16.70	13.40
Tree stress index (1 = healthy to 5 = dead)	avg	2.77	2.66	2.58	2.53	2.37	2.53
	std	0.62	0.75	0.70	0.59	0.82	0.67

shows the average (avg) and standard deviation (std) of the ground forest measurements.

4.2. Imagery acquisition

A multispectral sensor incorporating a Kodak Megaplus 1.4 black and white, 1320×1035 pixel format digital camera was used. The camera is entirely computer controlled, with a rotating filter wheel providing 8-bit data in up to eight spectral bands of >10 nm bandwidth between 430 and 1000 nm (King, 1995). The view angle of the camera was $\pm 9.1 \times 7.2^\circ$ using a 28-mm focal length lens. Imagery was acquired on September 7, 1995 (just before autumn leaf colour change) with 0.25, 0.5, and 1.0 m ground pixel spacings, 60% forward overlap, and a shutter speed of 1/300 s. The spectral bands used in this study were green (545–555 nm), red (665–675 nm), and near infrared (795–805 nm) corresponding to the major vegetation spectral absorption and reflectance regions in the visible and near-IR. Image motion due to aircraft translation during exposure was less than 1/2 pixel at all resolutions. The three spectral bands were aligned with a root mean squared error (RMS) of less than 0.22 pixel at each spatial resolution.

4.3. Extraction of image samples at the canopy and tree scales

Two scales of sampling were conducted to evaluate relations between image and forest variables.

(1) At the canopy-scale, an image sample was extracted over each plot's total area, including tree crowns and shadows to determine relations of average plot spectral and spatial variables with average plot canopy and individual tree measurements. The six plots were 200×200, 125×125, and 75×75 pixels for the 0.25, 0.5, and 1.0 m image resolutions, respectively. To minimize view angle effects on image brightness (e.g., bi-directional reflectance (BRDF) and optical effects), plots were extracted from images where they were located near the image centre. Each plot appeared near the centre of at least one image, as there was a significant amount of forward overlap. As additional verification, DN values for a plot extracted from two different images with view angles representing the maximum range for this imagery were found to not be significantly different (Student's *t*-test) in any of the spectral bands. Consequently, correction for spatial non-uniformity in image brightness was not applied. Atmospheric correction was not performed since the data were all acquired on the same clear day.

(2) At the tree-scale, image samples of between 25 and 324 pixels were extracted from each of four to six tree crowns per plot (total number of trees = 31) to analyze relationships between image measures and tree crown closure, stress index, and height. The other forest measures were not appropriate for this scale of study since they integrate information beyond the tree crown. The trees used in these analyses represented the typical ranges of these measures in the study area and all were positively identified in the field. Only the 0.25 and 0.5 m spatial resolutions were used, since it was not possible to visually delineate most of the tree crowns in the 1.0 m pixel image. Both the directly and diffusely illuminated portions were included in each delineated crown. Tests of precision were carried out by independently repeating the delineations three times to ensure that the mean and standard deviation of image brightness in each crown did not vary significantly due to delineation variations.

4.4. Spectral mixture analysis

Constrained linear spectral unmixing was performed on plot images from each of the three resolutions using an algorithm (Boardman, 1989) implemented in ISDAS (Imaging Spectrometer Data Analysis System; Staenz, Szeredi, & Schwarz, 1998). It decomposes the image spectra into a sub-pixel linear combination of endmember spectra. $N-1$ bands are required to spectrally unmix a scene with N endmembers. Therefore, a maximum of four endmembers could be extracted for these image data. Endmember spectra were selected using an automatic endmember extraction algorithm based on an iterative error analysis implemented in ISDAS by Neville, Staenz, Szeredi, Lefebvre, and Zur (1999). This method performs a series of linear constrained unmixing procedures with, as endmembers, the pixel spectra that minimize the unmixing error. The iterative process starts unmixing using the average spectrum of the image. The unmixing error, calculated for each pixel, is then used to determine the first endmember. The pixel spectrum with the largest error constitutes the first endmember since it is located at an extremity of the scatterplot. To select the pixels corresponding to this endmember, an angular tolerance of a few degrees (default = 2.5°) starting from the origin is used,

and the spectra of all pixels in this range are averaged. The user can define a maximum number of pixels to be averaged. The average spectrum of the image is then discarded and the process is repeated until the termination condition is reached, which is the number of endmembers requested by the user.

4.5. Extraction of image fractions

The iterative error analysis produced four endmembers in the following order: wood, shadow, tailings, and vegetation. Identification of the end members was achieved using the endmember fraction maps to locate their associated pixels in the field. The extraction of a wood end member was of particular interest. A single dead tree in Plot 2 provided many of the pixels of this end member. As large standing dead aspen trees did not occur elsewhere in the imagery and were relatively rare at the site, to test the relevance of including a wood end member in the analysis, the dead tree was masked from the imagery and automatic endmember selection was repeated. A wood endmember was still produced with a similar spectrum (as shown in a plot of principal components 1 and 2) but it consisted of pixels that were less pure (probably exposed branches on other trees) than when the dead tree was included in the imagery. The dead tree therefore provided more pure wood pixels and aided in identification of this endmember as wood. Consequently, it was retained for subsequent modelling. Fig. 3 shows three of the four-endmember fraction images at 0.5 m resolution. Their corresponding spectra are shown in Fig. 4. The tailings endmember was not included in forest modelling since it generally yielded a fraction of zero except at the tailings boundary.

In the forest canopy-scale analysis, image fractions for each endmember in each pixel were averaged over the given plots. This was repeated for the three image resolutions (0.25, 0.5, and 1.0 m). At the individual tree-scale, an average fraction for each endmember was calculated for each of the 31 tree crowns at the 0.25 and 0.5 m spatial resolutions.

4.6. Spatial analysis of image brightness and image fractions

Based on promising initial results of semivariance analysis using the NIR spectral band (Lévesque & King, 1999), and on the results of Treitz and Howarth (2000) showing semivariance to be spectrally dependent, semivariogram ranges and sills were calculated from the three raw spectral bands and from the three fraction images for both the forest canopy and individual tree crown sample data.

Twenty-four co-occurrence and grey-level difference vector texture measures (Haralick et al., 1973; PCI, 1994) were extracted from the three original bands and from the three fraction images at the three resolutions. A subset of four of these measures (mean, entropy, angular second moment, and contrast) were selected that were least correlated ($r < 0.79$) with each other and well correlated with the forest measures. The mean (MEA) measure is the average probability of grey level pair occurrence, entropy (ENT) measures the degree of organized patterns, angular second moment (ASM) indicates the degree of homogeneity of the values, and contrast (CON) measures the amount of local variation within the sample window. Because of the nature of their information, it is expected that when texture increases, MEA, ENT and CON will increase, and ASM will decrease. To determine the most suitable window size for canopy-scale texture analysis, windows were varied from 3×3 to 25×25 pixels with one extra window of large size also selected for each spatial resolution (total of 13 window sizes tested). This large window covered one quarter of the whole plot (99×99, 61×61, and 37×37 pixels for the 0.25, 0.5, and 1.0 m resolutions, respectively). The sampling direction was spatially invariant, that is the co-occurrence matrix was calculated from sample pairs in all directions, and the lag spacing was 1 pixel. From these tests the following pattern emerged: local texture derived from the smallest window sizes related best to forest variables such as individual tree crown closure and forest canopy closure, while regional texture derived from the largest window size related better to the visual forest stress index. Therefore, the smallest (3×3 pixels) and largest window sizes were retained at each resolution for regression analysis. For the individual tree crown samples, a window size of 3×3 was used, to minimize boundary effects, since a larger window size would calculate texture measures using too many pixels outside the sampled tree crown area.

4.7. Summary of image variables used in modelling

Table 2 summarises the image variables used in regression modelling of each forest variable at both canopy-scale and tree-scale. The image digital number (DN) and image fraction (IF) variables (VEG = vegetation, SHA = shadow, WOD = wood) are grouped into spectral, textural, and semivariogram variables. All are used in the canopy-scale analysis with the exception of the semivariogram variables at 0.25 m resolution (variables noted by: **). This spatial resolution was not found to be appropriate for semivariance analysis at the canopy-scale because image data become independent over short distances so that the ranges were reached within scene objects (tree crowns, gaps). At the individual tree crown-scale, the larger texture window and the 1.0-m resolution data were not used (variables noted by: *) because tree crowns were difficult to delineate and there were not enough pixels within many of the crowns to provide an adequate sample size.

4.8. Regression modelling of forest structure and health

Forward stepwise multiple regression was used to determine the combination of image variables that best models

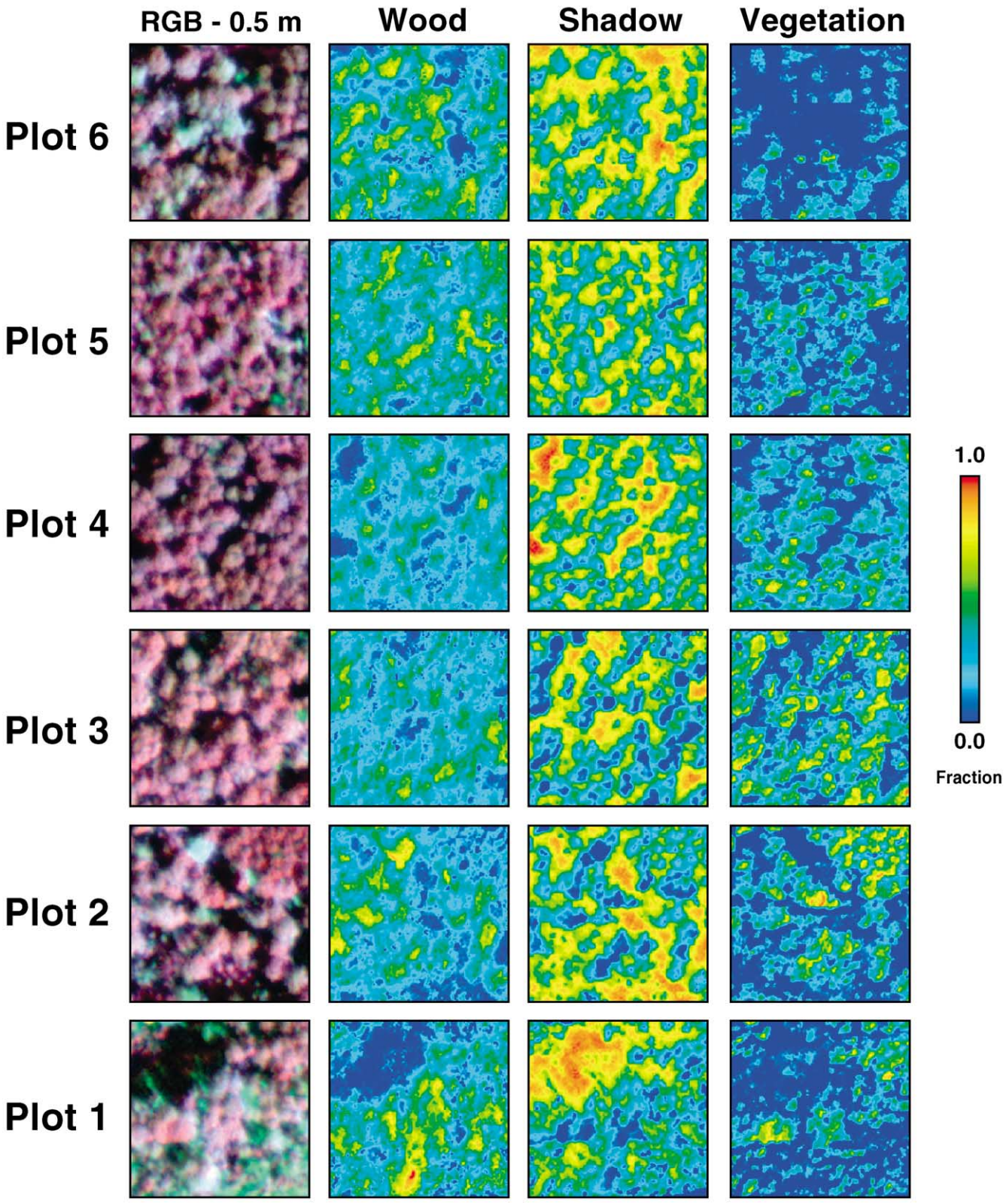

Fig. 3. Colour composites of the study plots and fraction images of the wood, shadow, and vegetation endmembers at 0.5 m resolution.

each forest measure. The forward method first selects the independent (image) variable that has the highest significant correlation with the dependent (forest) variable. The partial correlation coefficients of the remaining independent variables are then calculated and the variable with the highest significant coefficient is introduced next in the regression.

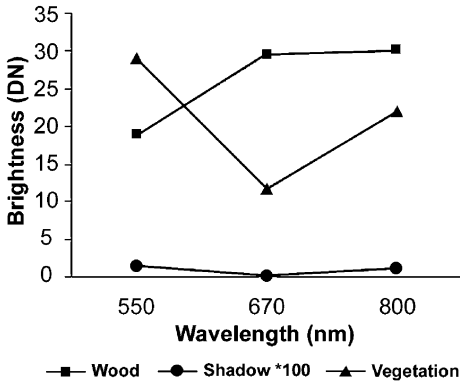

Fig. 4. Spectra of the wood, shadow, and vegetation endmembers at 0.5 m resolution.

This process is repeated until none of the partial correlation coefficients of the remaining independent variables is significant. The *F*-to-enter, the minimum significance level for a variable to be added to the model, was set at 0.05. The *F*-to-exit was set at 0.10. Prior to the multiple regression analysis, it was verified that all relationships were linear and all image variables were found to be normally distributed. To avoid multicollinearity amongst the dependent variables, a tolerance limit of the variance inflation factor [VIF = $1/(1-R^2)$] of 10 (Birkes & Dodge, 1993) was used, where R^2 is the multiple correlation of the variable with all other independent variables in the regression equation. Following regression, it was verified that all model residuals were distributed normally and presented no trend with the dependent variable.

In the canopy-scale regression analysis, the minimum number of plots should be about 15 (Draper & Smith, 1981). In this research, only six plots were used. When the research was designed, the methodology was adapted from King et al. (1992) and Yuan, King, and Vlcek (1991) where large plots were used for analysis of individual tree health with high-resolution imagery (similar to the tree-scale analysis of this study). It was not deemed possible to acquire field data for a greater number of plots of such large size near the time of the airborne data acquisition. However, since the six plots capture a wide range of forest conditions, particularly of canopy closure, the canopy-scale analysis was conducted. It was assured that the significant models did not include more than five independent variables, which is the number of degrees of freedom for six observations. In fact, all models included three or less variables. Final models were verified by a biostatistician (Pitt, 2001) and found to be stable and valid. Also, recognizing that the research was exploratory and empirical for a single local study site, the models were analyzed not in an absolute sense, but as relative comparisons amongst image variable type contributions. In this way, an assessment of the relative potential of each of the variable types could be made.

In canopy-scale sampling, a model was produced for each of the six forest measures at each of the three image resolutions. In crown-scale sampling each of the three forest measures (tree height, crown closure, stress index) was modelled at two resolutions (0.25 and 0.5 m). A total of 24 models were therefore evaluated from these combinations of forest variables, image resolutions, and image sampling scales. Five parameters are reported for each

Table 2
Summary of the image variables used at the canopy and tree crown-scales in the regression analysis

	0.25 m		0.50 m		1.0 m	
	DN	IF	DN	IF	DN	IF
Spectral variables	GREEN	VEG	GREEN	VEG	GREEN*	VEG*
	RED	SHA	RED	SHA	RED*	SHA*
	NIR	WOD	NIR	WOD	NIR*	WOD*
Texture variables	MEA-GREEN	MEA-VEG	MEA-GREEN	MEA-VEG	MEA-GREEN*	MEA-VEG*
	MEA-RED	MEA-SHA	MEA-RED	MEA-SHA	MEA-RED*	MEA-SHA*
	MEA-NIR	MEA-WOD	MEA-NIR	MEA-WOD	MEA-NIR*	MEA-WOD*
	ENT-GREEN	ENT-VEG	ENT-GREEN	ENT-VEG	ENT-GREEN*	ENT-VEG*
	ENT-RED	ENT-SHA	ENT-RED	ENT-SHA	ENT-RED*	ENT-SHA*
	ENT-NIR	ENT-WOD	ENT-NIR	ENT-WOD	ENT-NIR*	ENT-WOD*
	ASM-GREEN	ASM-VEG	ASM-GREEN	ASM-VEG	ASM-GREEN*	ASM-VEG*
	ASM-RED	ASM-SHA	ASM-RED	ASM-SHA	ASM-RED*	ASM-SHA*
	ASM-NIR	ASM-WOD	ASM-NIR	ASM-WOD	ASM-NIR*	ASM-WOD*
	CON-GREEN	CON-VEG	CON-GREEN	CON-VEG	CON-GREEN*	CON-VEG*
	CON-RED	CON-SHA	CON-RED	CON-SHA	CON-RED*	CON-SHA*
	CON-NIR	CON-WOD	CON-NIR	CON-WOD	CON-NIR*	CON-WOD*
Semivariogram variables	SILL-GREEN**	SILL-VEG**	SILL-GREEN	SILL-VEG	SILL-GREEN*	SILL-VEG*
	SILL-RED**	SILL-SHA**	SILL-RED	SILL-SHA	SILL-RED*	SILL-SHA*
	SILL-NIR**	SILL-WOD**	SILL-NIR	SILL-WOD	SILL-NIR*	SILL-WOD*
	RANGE-GREEN**	RANGE-VEG**	RANGE-GREEN	RANGE-VEG	RANGE-GREEN*	RANGE-VEG*
	RANGE-RED**	RANGE-SHA**	RANGE-RED	RANGE-SHA	RANGE-RED*	RANGE-SHA*
	RANGE-NIR**	RANGE-WOD**	RANGE-NIR	RANGE-WOD	RANGE-NIR*	RANGE-WOD*

* Variables used at canopy-scale only. **Variables used at individual tree-scale only. VEG = vegetation, SHA = shadow, WOD = wood, MEA = mean, ENT = entropy, ASM = angular second moment, CON = contrast.

model: (1) R^2, the proportion of total variance about the mean that is explained by the image variables in the regression, (2) adjusted R^2, which adjusts R^2 for the number of degrees of freedom of the model and is a better measure for comparing models of different numbers of x variables, (3) the change in R^2 contributed by each image variable in the model, (4) the significance of each predictor variable, and (5) the overall significance of the model. The results are then aggregated to evaluate the relative contributions of each variable type (raw DN, IF, DN-TEX, IF-TEX, DN-SEMI, IF-SEMI) to the significant models based on: (1) the average contribution (R^2 change) of each variable type to the best models, determined by dividing the sum of its R^2 values in the models by the number of best models in which it was present, (2) the frequency of occurrence of each variable type as the primary (first entered) variable in the models.

5. Results and discussion

In the following sections, for brevity, only the regression models with the highest adjusted R^2 are discussed. In addition, tables of model results are presented only for the 0.5 m pixel spacing as this resolution produced equally or more significant models for each forest variable than the other two resolutions. As common image variables and trends were found between models of each forest variable, each of the 'best' models is not discussed individually.

5.1. Models developed using image samples extracted from the whole plot (canopy-scale)

Table 3 shows the best modelling results for each forest variable at the canopy scale in 0.5 m pixel imagery. The sign of each independent variable is given along with the statistical parameters discussed above.

5.1.1. Model interpretation

In the more damaged plots, canopy closure, stem density, and individual tree crown closure tended to be lower than in healthier plots, while tree crown size and the stress index were higher. All of these, except crown closure, were well modelled using canopy scale samples. In the significant models at all resolutions, the image variables followed very consistent trends. They were almost all spatial transformations of either image brightness or image fractions. Of the most significant variable types, semivariance range of the green and NIR bands and the wood fraction consistently increased with damage/openness. The range of the vegetation fraction was a minor variable in models of crown size (1% of model variance) and tree height (17% of model variance). The range measures the distance of major object brightness, in this case corresponding to larger and fewer trees and gaps, as well as more exposed wood in damaged conditions.

Texture measures were second most significant in these models and the primary variables at 0.25 m resolution (semivariance variables had not been extracted from the 0.25 m imagery). The most important of these were: (1) decreased canopy closure associated with increased texture (semivariogram sill) in the red band due to increased brightness variability from mixing of understory and overstory contributions, and (2) increased stress index associated with decreased shadow fraction co-occurrence texture because shadows become less well defined as discrete brightness entities with increasing openness. Texture of the wood fraction and NIR band were minor variables in models of stem density and tree height, respectively.

5.1.2. Comparison of the contribution of each image variable type to the models

There were 25 image variables used in 13 'best' models at the forest canopy-scale for all resolutions. Fig. 5a shows that the contribution (average R^2) of raw image brightness (DN) and image fractions (IF) to the variance of these models was much less than their associated spatial transformations. Of

Table 3
Results of forward stepwise multiple regression of forest variables (dependent variables) and image variables (independent variables) for forest canopy samples and 0.5 m pixel imagery

Forest measure	Model type	Model variables	R^2	Adjusted R^2	R^2 change	Predictor significance	Overall significance
Forest canopy closure	DN	− RANGE/550	0.98	0.96	0.72	0.00	0.00
		− SILL/670			0.26	0.01	
Forest stem density	DN and IF	− RANGE/550	1.00	0.99	0.69	0.01	0.01
		− RANGE/800			0.27	0.01	
		− ENT(3)/WOD			0.04	0.04	
Tree crown size	DN and IF	+ RANGE/800	1.00	1.00	0.99	0.00	0.00
		+ RANGE/VEG			0.01	0.02	
Tree height	DN and IF	+ RANGE/800	1.00	0.99	0.80	0.00	0.00
		+ RANGE/VEG			0.17	0.01	
		+ ASM(5)/800			0.03	0.03	
Tree crown closure	IF	− RANGE/WOD	0.68	0.60	0.68	0.04	0.04
Tree stress index	DN and IF	− ENT(5)/SHA	0.99	0.98	0.80	0.00	0.00
		− 550			0.19	0.01	

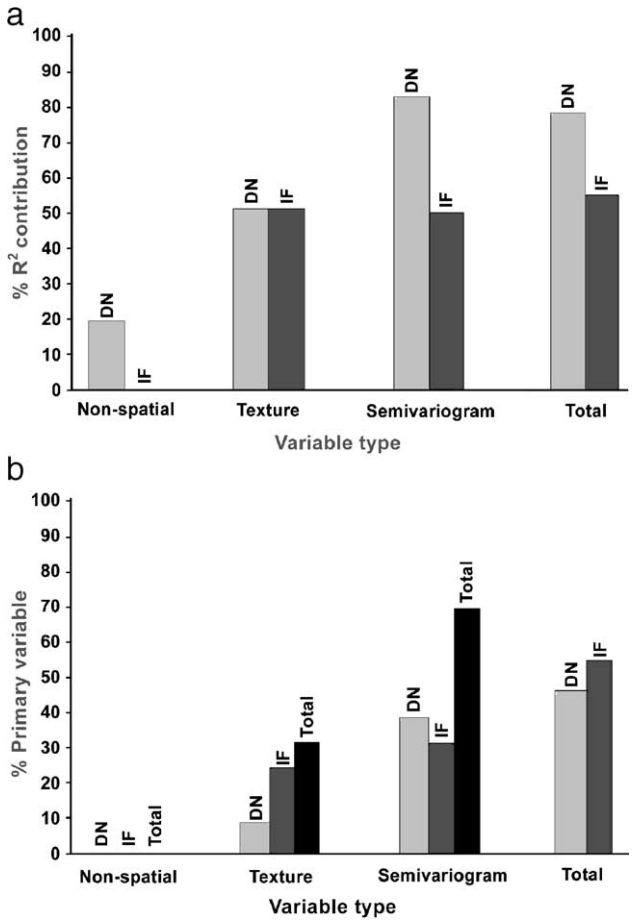

Fig. 5. (a) Average R^2 contribution per model at the canopy scale. Values correspond to the sum of R^2 values divided by the number of models the set of variables contributes to. (b) Proportion (%) of each variable type first entered in the most significant models at the canopy scale.

the spatial transformations, semivariance variables (most often the range) of the DN values contributed much more to model variance than DN texture variables. For the IF variables, semivariance and texture variables contributed about equally to the best models. Fig. 5b shows that spatial transforms of DN and IF variables completely dominated as the primary variables in all models. Semivariance variables derived from both IF and DN formed the bulk of these (90% of models where range was available as an input), but the number of primary texture variables was not insignificant. Overall, the best information contained in raw image brightness was in its derived semivariogram variables, these being mostly range, while information contained in image fractions was approximately equally divided between their texture and semivariogram derived variables.

The above interpretations are based on an analysis with a limited number of plots. Two additional tests were conducted to determine if these interpretations remained consistent with: (1) a more strict significance level ($p<0.01$, significant $R^2>0.84$), and (2) increased numbers of samples for the canopy closure variable, whose locations for many of the within plot measurements ($n=23$) could be determined in the imagery. In the first test, with $p<0.01$, half of the models at the 0.5 and 0.25 m resolutions were significant while only one model (stress index) was significant at the 1.0 m resolution. All consisted of spatially transformed variables, and at 0.25 m resolution all significant models (canopy closure, crown size, stress index) included texture of the wood fraction as the only predictor. For the second test, a model of canopy closure produced with 23 samples ($R^2=0.55$, $p=0.001$) also consisted of only textures of the vegetation and wood fractions plus the 550 nm band. These results reinforce two findings presented earlier in this paper: (1) the wood fraction, which can only be extracted using such high-resolution imagery is a critical variable, and (2) spatially transformed DN and IF variables have strong potential in such modelling. These points are demonstrated in Fig. 6. It shows two plots that had a similar and relatively high average wood fraction. In Plot 3, the wood fraction was distributed throughout the canopy whereas in Plot 4, the wood fraction is clustered more on a few dead trees and/or large dead branches. The differences between these plots are evident more in the spatial properties of the wood fraction than in the amount of wood fraction. A second example that was observed is that higher shadow fraction and lower vegetation fraction may result from either a few large openings or from many small gaps spread over the canopy. While the image fractions for these two conditions may be similar, their spatial patterns are captured in either the semivariance or texture measures.

5.2. Models developed using image samples extracted from individual tree crowns (crown-scale)

Table 4 shows the best models for crown-scale analysis of tree closure, height, and stress index using the 0.5 m pixel imagery.

5.2.1. Model interpretation

Following the logic of the canopy-scale analysis, trees with lower crown closure were associated with a greater stress index and were often taller (although this association is weak). All image variables in the best models were measures of texture; semivariance range and sill did not contribute significantly. More open, damaged trees exhibited reduced texture in the green and NIR bands, reduced texture in the vegetation and shadow fractions, and increased texture of the wood fraction. As damage in a crown increases, within crown shadows become more diffuse and background vegetation contributions increase, resulting in decreased textures. The wood fraction increases with damage, probably because exposed dead branches are clustered in various parts of the crown.

5.2.2. Comparison of the contribution of each image variable type to the models

For the six best models, texture of image brightness and texture of image fractions accounted for most of the var-

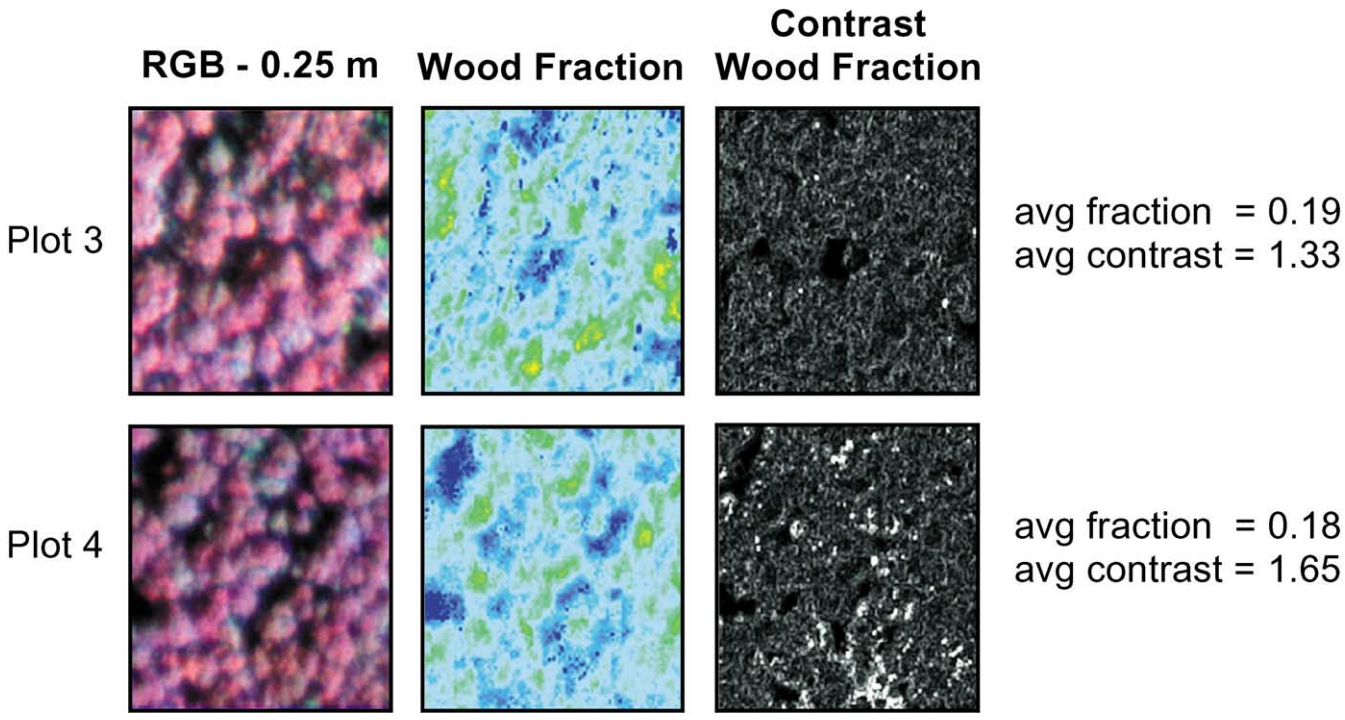

Fig. 6. Colour composites of Plot 3 and Plot 4, their average wood fraction and their respective wood fraction contrast texture at 0.25 m resolution.

iance (Fig. 7a), although image fractions contributed significantly. Raw image brightness was again negligible in its contributions to model variance and semivariance variables played only a minor role. Texture variables were also the primary variables in five of these models (Fig. 7b). An image fraction variable (vegetation) was the primary variable in one model (crown closure—0.25 m).

5.2.3. Evaluation of spatial resolutions

In canopy-scale sampling, 0.5 m resolution models of the six forest variables accounted for an average of 95% of model variance. This was more than at the 1.0 m resolution (91%) and less than the 0.25 m resolution (98%). Semivariogram parameters (mostly range) dominated at 0.5 and 1.0 m resolutions. Texture dominated the models at 0.25 m resolution (but semivariance variables were not used in canopy sampling at this resolution). In crown-scale sampling, 0.5 m resolution models of the three forest variables evaluated accounted for an average of 55% while models derived from 0.25 m resolution images accounted for 53% variance. Thus, overall, if only one spatial resolution can be used, 0.5 m is the best choice. It allows extraction of the semivariogram range related to tree size and configuration (0.25 m imagery ranges were often within crowns), provides greater ground coverage, is easier to mosaic and geo-reference, and provides models of approximately equal quality to those of 0.25 m imagery.

Table 4
Results of forward stepwise multiple regression of forest variables (dependent variables) and image variables (independent variables) for tree crown samples and 0.5 m pixel imagery

Forest measure	Model type	Model variables	R^2	Adjusted R^2	R^2 change	Predictor significance	Overall significance
Tree height	DN	− CON(3)/550	0.14	0.11	0.14	0.04	0.04
Tree crown closure	DN and IF	− ASM(3)/550	0.79	0.76	0.51	0.00	0.00
		+ MEA(3)/VEG			0.16	0.00	
		− CON(3)/WOD			0.06	0.00	
		+ CON(3)/SHA			0.06	0.01	
Tree stress index	DN and IF	− ENT(3)/550	0.72	0.67	0.37	0.00	0.00
		− MEA(3)/VEG			0.10	0.00	
		+ CON(3)/WOD			0.08	0.00	
		− ENT(3)/800			0.11	0.00	
		+ ASM(3)/VEG			0.06	0.03	

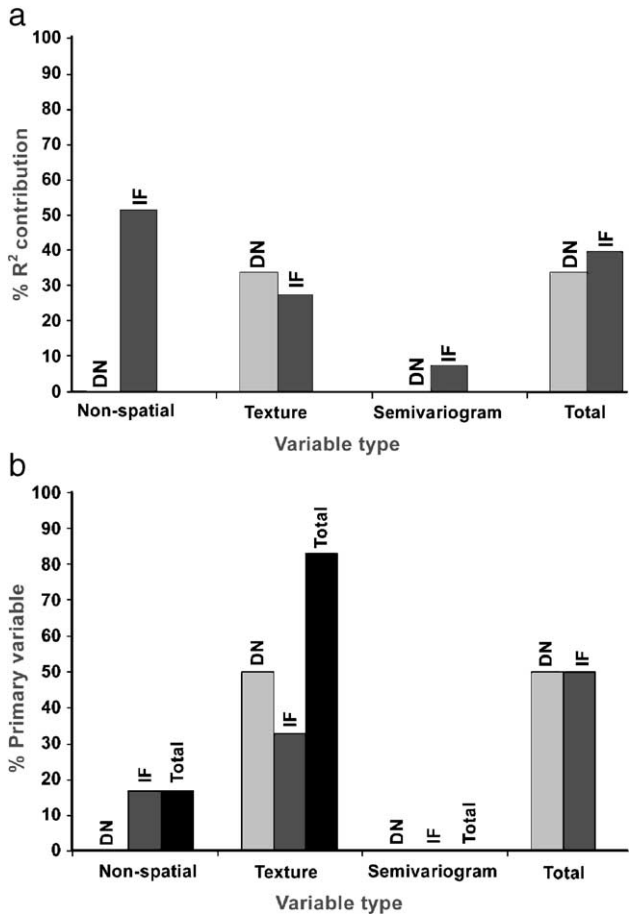

Fig. 7. (a) Average R^2 contribution per model at the crown scale. Values correspond to the sum of R^2 values divided by the number of models the set of variables contributes to. (b) Proportion (%) of each variable type first entered in the most significant models at the crown scale.

The results of these analyses indicate that high spatial detail is very useful in forest modelling. In comparing models of the stress index at the three resolutions, as pixel spacing decreased (from 1.0 to 0.25 m), the stress index was detected through more subtle image information. It was best detected at 1.0 m resolution using the distance of major brightness variation between crowns and shadows (semivariogram range), at 0.5 m resolution using the texture of the shadow fraction (a component of the total image brightness), and at 0.25 m resolution using the texture of the wood fraction. As stated earlier, the wood endmember, requires very high-resolution imagery to be resolved. The linear morphology of branches and stems as seen from above does not produce pure wood pixels at the 0.5 and 1.0 m resolutions. For such high detail related to tree stress, the 0.25 m is more suited.

6. Conclusions

The main goal of this research was to develop and compare image-based models of forest structure and health from spectral and spatial information. This was accomplished at two scales of study (forest canopy and individual tree) using high spatial resolution multispectral imagery (0.25, 0.5, 1.0 m) acquired in three 10 nm spectral bands (green, red, NIR). This paper introduced evaluation of spatial information (semivariance range and sill, co-occurrence texture) in spectrally unmixed image fractions of vegetation, shadow and wood. This information was found to be useful in forest structure and health modelling and complementary to spatial information derived from image brightness. Overall, spatial information dominated all models—image brightness and image fractions contributed very little to model variance. Semivariogram range was the single most important variable but textures of image brightness and fractions were also significant, particularly at 0.25 m resolution. Of the three resolutions evaluated, 0.5 m pixel spacing provided models that were consistently as good as, or better than the other two resolutions. Canopy-scale sampling was shown to be more suitable for all forest variables except individual tree closure where crown samples are required.

Models developed here are initial and empirical, having been developed on a single small study area. However, the method can be adapted to different forest canopy ecosystems for applications such as habitat and forest structure mapping, and mine site reclamation/recovery monitoring. For example, current research by the first author to monitor re-vegetation of mine tailings at another site is incorporating hyperspectral image fraction textures. Because of high acidity and high variation in tailings chemical composition, vegetation grows sporadically on these sites. Fractional texture of dry and green vegetation, exposed tailings, and lime helps to identify problem areas.

Acknowledgements

This research was funded by the Natural Sciences and Engineering Research Council of Canada through a grant to D. King. Falconbridge allowed access to the KamKotia Mine site, and the Ontario Ministry of Natural Resources in Timmins provided some field equipment. Air Focus of Chicoutimi provided airborne data acquisition capabilities. Dr. Doug Pitt of the Canadian Forest Service reviewed and advised on the regression procedure. Chris Butson, Alex Chichagov, Fons Schellekens, and Nick Walsworth provided valuable field assistance.

References

Atkinson, P. M., & Lewis, P. (2000). Geostatistical classification for remote sensing: an introduction. *Computers and Geosciences*, *26*, 361–371.

Berberoglu, S., Lloyd, C. D., Atkinson, P. M., & Curran, P. J. (2000). The

integration of spectral and textural information using neural networks for land cover mapping in the Mediterranean. *Computers and Geosciences*, *26*, 385–396.

Birkes, D., & Dodge, Y. (1993). *Alternative methods of regression*. John Wiley & Sons, New York. 223 pp.

Boardman, J. W. (1995). Analysis, understanding and visualization of hyperspectral data as convex sets in n-space. *SPIE*, *2480*, 14–21.

Boardman, J. W. (1989). Inversion of imaging spectrometry data using singular value decomposition. *Proceedings of the 1989 International Geoscience and Remote Sensing Symposium (IGARSS '89) and the 12th Canadian Symposium on Remote Sensing. Vancouver, BC, Canada, vol. 4* (pp. 2069–2072).

Bowers, W. W., Franklin, S. E., Hudak, J., & McDermid, G. J. (1994). Forest structural damage analysis using image semivariance. *Canadian Journal of Remote Sensing*, *20*, 28–36.

Butson, C., & King, D. J. (1999). Semivariance analysis of forest structure and remote sensing data to determine an optimal sample plot size. *Proceedings 4th International Airborne Remote Sensing Conference and Exhibition (Env. Res. Inst. of Michigan)/21st Canadian Symposium on Remote Sensing (Can. Rem. Sens. Soc.), Ottawa, Ontario, June 21–24, vol. II* (pp. 155–162).

Carlson, T. N., & Ripley, D. A. (1997). On the relation between NDVI, fractional vegetation cover, and leaf area index. *Remote Sensing of Environment*, *62*, 241–252.

Carter, G. A. (1994). Ratios of leaf reflectance in narrow wavebands as indicators of plant stress. *International Journal of Remote Sensing*, *15*(3), 697–703.

Coops, N., & Culvenor, D. (2000). Utilizing local variance of simulated high spatial resolution imagery to predict spatial pattern of forest stands. *Remote Sensing of Environment*, *71*, 248–260.

Cosmopoulos, Y. (2000). *Temporal analysis of forest change at an abandoned mine site using high-resolution remote sensing*. M.Sc. thesis, Carleton University, Ottawa-Carleton Geoscience Centre, 164 pp.

Cosmopoulos, Y., & King, D. J. (2001). Multivariate analysis of forest change at an abandoned mine site using airborne digital camera imagery. *Proceedings 18th Biennial Workshop on Color Photography and Videography in Resource Assessment (Am. Soc. Photogramm. And Rem. Sens.), Amherst, Massachusetts, May 16–18. CD-ROM publication*, In press.

Curtiss, B., & Ustin, S. L. (1989). Parameters affecting reflectance of coniferous forest in the region of chlorophyll pigment absorption. *Proc. of the 12th Canadian Symposium on Remote Sensing, IGARSS'89. Vancouver, July 10–14, vol. 4* (pp. 2633–2636).

Draper, N. R., & Smith, H. (1981). *Applied regression analysis* (2nd ed.). John Wiley & Sons, New York. 709 pp.

Gamon, J. A., Field, C. B., Goulden, M. L., Griffin, K. L., Hartley, A. E., Joel, G., Peñuelas, J., & Valentini, R. (1995). Relationshps between NDVI, canopy structure, and photosynthesis in three Californian vegetation types. *Ecological Applications*, *5*(1), 28–41.

Haralick, R. M., Shanmugan, K., & Dinstein, I. (1973). Textural features for image classification. *IEEE Transactions on Systems, Man, and Cybernetics*, *SMC-3*, 610–621.

King, D. J. (1995). Airborne multispectral digital camera and video sensors: a critical review of system designs and applications. *Canadian Journal of Remote Sensing, Special Issue on Aerial Optical Remote Sensing*, *21*(3), 245–273.

King, D. J., Yuan, X., & Sankey, A. (1992). Evaluation of the accuracy and cost-effectiveness of airborne multispectral videography in sugar maple decline assessment. *Proc.15th Canadian Symposium on Remote Sensing. Canadian Remote Sensing Society, Toronto, ON, June 1–4* (pp. 138–143).

Lévesque, J., & King, D. J. (1999). Airborne digital camera image semivariance for evaluation of forest structural damage at an acid mine site. *Remote Sensing of Environment*, *68*, 112–124.

Luther, J. E., & Carroll, A. L. (1999). Development of an index of Balsam fir vigour by foliar spectral reflectance. *Remote Sensing of Environment*, *69*, 241–252.

McDonald, A. J., Gemmel, F. M., & Lewis, P. E. (1998). Investigation of the utility of spectral vegetation indices for determining information on coniferous forests. *Remote Sensing of Environment*, *66*, 250–272.

Merzlyak, M. N., Gitelson, A. A., & Zur, Y. (1999). Remote detection of leaf senescence. *Proceedings of the 4th International Airborne Remote Sensing Conference and Exhibition/21st Canadian Symposium on Remote Sensing, Ottawa, ON, June 21–24, vol. 2* (pp. 197–203).

Neville, R. A., Staenz, K., Szeredi, T., Lefebvre, J., & Hauff, P. (1999). Automatic endmember extraction from hyperspectral data for mineral exploration. *Proceedings of the 4th International Airborne Remote Sensing Conference and Exhibition/21st Canadian Symposium on Remote Sensing, Ottawa, Ontario, Canada, 21–24 June*.

Olthof, I., & King, D. J. (1997). Evaluation of textural information in airborne CIR digital camera imagery for estimation of forest stand leaf area index. *Proc. of the 15th North American Symposium on Small Format Aerial Photography (ASPRS), Cloquet, MN, Oct. 12–15* (pp. 154–164).

Olthof, I., & King, D. J. (2000). Development of a forest health index using multispectral airborne digital camera imagery. *Canadian Journal of Remote Sensing*, *26*(3), 166–176.

PCI (1994). *Using PCI software (PCI 6.2)*. Richmond Hill, Ontario, Canada: PCI.

Peddle, D. R., Hall, F. G., & LeDrew, E. F. (1999). Spectral mixture analysis and geometric-optical reflectance modelling of boreal forest biophysical structure. *Remote Sensing of Environment*, *67*, 288–297.

Peddle, R. D., Davidson, D. P., Johnson, R. L., & Hall, R. J. (1999). Airborne image texture and mixture analysis of a forest scale continuum: a comparison with NDVI biophysical estimates, Kananaskis Alberta. *Proceedings of the 4th International Airborne Remote Sensing Conference and Exhibition/21st Canadian Symposium on Remote Sensing, Ottawa, Ontario, 21–24 June, vol. 2* (pp. 848–855).

Pinty, B., & Verstraete, M. M. (1992). GEMI: a non-linear index to monitor global vegetation from satellite. *Vegetatio*, *101*, 15–20.

Pitt, D. (2001). *Personal communication*. Natural Resources Canada, Canadian Forest Service, Sault Ste-Marie, Ontario, November.

Piwowar, M. P., & Peddle, D. R. (1999). Assessing annual forest ecological change in western Canada using temporal mixture analysis of regional scale AVHRR imagery over a 14-year period. *Proceedings of the 4th International Airborne Remote Sensing Conference and Exhibition/21st Canadian Symposium on Remote Sensing, Ottawa, Ontario, 21–24 June, vol. 2* (pp. 91–97).

Salisbury, F. B., & Ross, C. W. (1985). *Plant physiology* (3rd ed.). Belmont, CA: Wadsworth, 540 pp.

Seed, E. D., & King, D. J. (2002). Boreal mixed wood LAI estimation using high-resolution digital camera shadow brightness and shadow fraction. *Canadian Journal of Remote Sensing, Special Issue on LAI*, (Accepted 08/02).

Staenz, K., Szeredi, T., & Schwarz, J. (1998). ISDAS—a system for processing/analyzing hyperspectral data. *Canadian Journal of Remote Sensing*, *24*, 99–113.

Treitz, P., & Howarth, P. (2000). High spatial remote sensing data for forest ecosystem classification: an examination of spatial scale. *Remote Sensing of Environment*, *72*, 268–289.

Turner, D. P., Cohen, W. B., Kennedy, R. E., Fassnacht, K. S., & Briggs, J. M. (1999). Relationships between leaf area index and LANDSAT TM spectral vegetation indices across three temperate zone sites. *Remote Sensing of Environment*, *70*, 52–68.

Wallace, C. S. A., Watts, J. M., & Yool, S. R. (2000). Characterizing the spatial structure of vegetation communities in the Mojave desert using geostatistical techniques. *Computers and Geosciences*, *26*, 397–410.

Walsworth, N. A., & King, D. J. (1999). Image modelling of forest changes associated with acid mine drainage. *Computers and Geosciences*, *25*, 567–580.

Wulder, M., Franklin, S., & Lavigne, M. (1996). Statistical texture properties of forest structure for improved LAI estimates from casi. *Proc. of the 26th International Symposium on Remote Sensing of Environment/18th Annual Symposium of the Canadian Remote Sensing Society, 25–29 March, Vancouver, BC* (pp. 161–164).

Yoder, B. J., & Waring, R. H. (1994). The normalized difference vegetation index of small Douglas-fir canopies with varying chlorophyll concentrations. *Remote Sensing of Environment*, *49*, 81–91.

Yuan, X. Y., King, D. J., & Vlcek, J. (1991). Sugar maple decline assessment based on spectral and textural analysis of multispectral aerial videography. *Remote Sensing of Environment*, *37*, 47–54.